Journal of Power Sources 238 (2013) 74–80

Contents lists available at SciVerse ScienceDirect

Journal of Power Sources

journal homepage: www.elsevier.com/locate/jpowsour

High-temperature stability of alumina containing nickel–zirconia cermets for solid oxide fuel cell anodes

Himeko Orui [a,b,*], Reiichi Chiba [a], Kazuhiko Nozawa [a], Hajime Arai [a], Ryoji Kanno [b]

[a] NTT Energy and Environment Systems Laboratories, 3-1 Morinosato-Wakamiya, Atsugi-shi, Kanagawa 243-0198, Japan
[b] Department of Electronic Chemistry, Tokyo Institute of Technology, 4259, Nagatsuta-cho, Midori-ku, Yokohama-shi, Kanagawa 226-8502, Japan

HIGHLIGHTS

- The mechanism of the stability of Ni–SASZ under SOFC operation condition was studied.
- The nickel aggregation was suppressed by adding Al_2O_3 to the NiO–ScSZ anode.
- The $NiAl_2O_4$ spinel phase was confirmed from the XRD of as sintered anodes with Al_2O_3.
- The TG measurement revealed that the $NiAl_2O_4$ wasn't reduced easily at 800 °C.
- The defect spinel phase of $NiAl_{10}O_{16}$ remained after 600 h reduction of $NiAl_2O_4$ at 800 °C.

ARTICLE INFO

Article history:
Received 16 January 2013
Received in revised form
11 March 2013
Accepted 12 March 2013
Available online 21 March 2013

Keywords:
Solid oxide fuel cell
Anode
Nickel–zirconia cermets
Nickel aluminate
Conductivity

ABSTRACT

The long-term stability of anode cermets for solid oxide fuel cells (SOFC) was studied for the composites NiO/scandia stabilized zironia (ScSZ) and NiO/scandia-alumina stabilized zirconia (SASZ). Heat treatment at 800 °C over 600 h resulted in gradual conductivity degradation for the NiO/ScSZ composites, while no significant changes were found for the NiO/SASZ composites. The conductivity drop was caused by an aggregation of Ni in the cermet matrix at high temperatures, and the addition of alumina to the cermet matrix protected the Ni segregation and improved the long-term stability. The effect of the alumina was examined using a sintered model anode of the NiO/ScSZ system. Although the initial conductivity decreased with increasing alumina content, an anode with an alumina content of 3 mol% showed no conductivity degradation during heating over 600 h. The initial conductivity drop was caused by a $NiAl_2O_4$ spinel formed during the initial sintering process. The spinel phase was reduced at 800 °C and transformed slowly into metastable $NiAl_{10}O_{16}$, which contributed to the long-term stability of the alumina composite anode cermets.

1. Introduction

A solid oxide fuel cell (SOFC) is a promising power generation system because of its high energy conversion efficiency and low environmental pollution. Of the several types of the cell configuration proposed for SOFCs, anode supported cells have been widely investigated because of their low internal ohmic resistance [1–5]. However, the long-term stability of the cell components is still an important requirement for an SOFC, because the cells are usually operated at a high temperature of 800–1000 °C [6–8].

In an anode supported SOFC, the anode is composed of electronic and ionic conducting components, and occupies most of the cell volume to satisfy the mechanical strength of the cell. Nickel–zirconia cermets are the most commonly used materials for SOFC anodes. Nickel functions as an electrically conductive catalyst in a cermet anode because of its good electrical conductivity, its catalysis of hydrogen oxidation and its stability in a reducing atmosphere [3,9]. Yttria stabilized zirconia (YSZ) is widely used as an oxide ion conducting component for cermet anodes. Scandia stabilized zirconia (ScSZ) or scandia–alumina stabilized zirconia (SASZ) is also employed for the cermets because of its high ionic conductivity at an intermediate temperature of around 800 °C [10–12].

Electrical conductivity is an important parameter for anode cermets. The cermets are usually obtained by mixing NiO and zirconia powder and then reducing the NiO to nickel metal at high

* Corresponding author. NTT Energy and Environment Systems Laboratories, 3-1, Morinosato-Wakamiya, Atsugi-shi, Kanagawa 243-0198, Japan. Tel.: +81 46 240 2711; fax: +81 46 270 2702.
E-mail address: orui.himeko@lab.ntt.co.jp (H. Orui).

0378-7753/$ – see front matter © 2013 Elsevier B.V. All rights reserved.
http://dx.doi.org/10.1016/j.jpowsour.2013.03.056

temperature in a reduction gas atmosphere containing hydrogen. A nickel–nickel connection is then formed, and the cermet exhibits electrical conductivity as an electrode. The electrical conductivity of a cermet anode depends largely on the ratio with which it is mixed with nickel and zirconia, and a Ni content exceeding 40 vol% is reported to be necessary to provide sufficiently high electric conductivity for the anode [13,14].

Long-term stability is another important factor as regards anode cermets. It has been reported that the anode degrades when the nickel particles in the cermets are sintered during high temperature operation [15]. To achieve the long-term stability of the high electric conduction state, a good zirconia channel should be formed to prevent nickel from sintering in the cermets and the nickel–nickel connection from becoming weakened and/or cut off under high temperature operation [7,16]. There are several parameters that affect the nickel sintering phenomena these include the particle size and the ratio of nickel and zirconia in the mixture [16,17]. The wetting behavior is also an important factor; a poor wettability between Ni and YSZ causes nickel sintering [18], and the composition of the ceramic component affects the wetting properties [19,20].

To improve the long-term stability of the cermet anode, a composite structure with mixed oxides has been proposed. Shiratori et al. fabricated $Ni_{1-x-y}Mg_xAl_yO$–ScSZ anodes and indicated the possibility of a Ni–zirconia cermet containing additive oxides [21]. They reported that small Ni particles formed by the reduction were stable against sintering.

The aim of this study is to develop a cermet anode that has stable electrical properties during operation at intermediate temperatures. For this purpose, we fabricated anode cermets with different zirconia compositions (ScSZ or SASZ) and investigated the long-term stability of the electrical conductivity. In particular, we focused on the effect of Al_2O_3 in the NiO–ScSZ on the electric conductivity and on nickel sintering in the operating atmosphere. The nickel sintering mechanism during the sintering and operating procedure is discussed based on the model composite systems.

2. Experimental

2.1. Sample preparation

A mixture consisting of 60 wt% NiO and 40 wt% zirconia was used for the cermet samples. As the zirconia powder, we used 10 mol% Sc_2O_3 stabilized ZrO_2 (ScSZ, Daiichi Kigenso Kagaku Kogyo Co.) or 10 mol% Sc_2O_3 and 1 mol% Al_2O_3 stabilized ZrO_2 (SASZ, Daiichi Kigenso Kagaku Kogyo Co.). The average particle diameters and surface areas were respectively 0.53 μm and 8.9 $m^2\ g^{-1}$ for ScSZ and 0.37 μm and 10.1 $m^2\ g^{-1}$ for SASZ. The NiO powder had an average particle diameter of 3.6 μm, with a surface area of 0.97 $m^2\ g^{-1}$. To confirm the effect of the addition of alumina on the characteristics of the anode cermets, 0.3–6 mol% of Al_2O_3 powder (99%purity, Kanto Kagaku) was added to the ScSZ and NiO–zirconia composites were prepared. These green sheets were fabricated by the doctor blade method and laminated until an appropriate thickness was obtained. They were then sintered at 1300 °C for 2 h in air atmosphere.

2.2. Measurements

2.2.1. Electrical measurements

For the electrical conductivity measurements, the sintered NiO–zirconia composites were cut to a size of 50 × 5 × 1 mm. For the measurements, four Pt wires were wrapped around the sample and Pt paste was applied to ensure good contact. The measurements were performed using the dc four-probe method. The sample terminal voltage was monitored during the reduction procedure. The sample terminal voltages became stable 10–15 min after the dry H_2 gas had been introduced. Then the electrical conductivity was measured by monitoring the voltage at the inner terminals while supplying current to the outer terminals. A long-term stability test was performed at 800 °C by supplying a current of 2.5 A cm^{-2}. During the measurements a reduction gas consisting of 20% H_2 in N_2 was supplied at a flow rate of 250 ml min^{-1}.

2.2.2. Micro-structure analysis

The porosity of the NiO–zirconia composites was measured with a mercury porosimeter (Shimadzu AutoPore 9520). The microstructures of the Ni–zirconia cermets were observed with a scanning electron microscope (SEM) (S-3200H, Hitachi High Technology or ULTRA55, Carl Zeiss). The elemental distributions of the samples after long-term measurement were analyzed with an energy dispersive spectrometer (EDS) (QUANTAX400, BRUKER).

2.2.3. X-ray diffraction measurements

The reactivity between NiO and Al_2O_3 during sintering was evaluated with X-ray diffraction measurements. An 1:1 M ratio mixture of NiO and Al_2O_3 powder was heated at 1300 °C for 2 h. We call this heat-treated powder mixture N-A-1300. The N-A-1300 was then reduced at 800 °C with various reduction times.

The crystal structure of the samples was analyzed with a Rint 2000/PC X-ray diffractometer (Rigaku). The high voltage and filament current for the Cu target were 30 kV and 100 mA, respectively. The diffraction angle 2θ was scanned at a rate of 1.0 or 2.0 s/step, from 10 to 90°with a step size of 0.04°. The molar ratio of each phase in the samples was evaluated by Rietveld analysis (RIQAS, Materials Data Inc. Company). The crystal system and initial unit cell parameters of the phases were taken from the Inorganic Crystal Structure Database (ICSD).

2.2.4. Thermogravimetric analysis

Thermogravimetric (TG) analysis was used to monitor the reduction behavior of the NiO–zirconia composites and N-A-1300. We employed two reduction conditions during the TG analysis. One was that the sample was reduced as the temperature increased to the operating temperature and the other was that the sample was reduced once the operating temperature had been reached. We refer to the former reduction approach as constant temperature ramp rate (CTR) reduction and to the latter as constant temperature (CT) reduction. The weight loss during CTR and CT reduction was determined by TG analysis (TG/DTA 320 Seiko Instruments). During the CTR reduction, the samples were heated to 800 °C at a constant ramp rate of 10 °C min^{-1} in a reduction gas atmosphere. The reduction gas consisted of a 5% H_2/N_2 mixture and was supplied at a flow rate of 200 ml min^{-1}. On the other hand, the CT reduction TG analysis was carried out as follows. The sample was first heated to 800 °C at a rate of 10 °C min^{-1} in an inert atmosphere of N_2. The sample was then held at 800 °C for over 4 h in a reduction gas consisting of a 5% H_2/N_2 mixture, and subsequently cooled to room temperature in a 5% H_2/N_2 mixture at a rate of 10 °C min^{-1}. Here, the total gas flow rate was 200 ml min^{-1}.

3. Results and discussion

3.1. Stability of electric conductivity of nickel–zirconia cermets with different zirconia compositions

Fig. 1 shows the conductivity changes in Ni–ScSZ and Ni–SASZ during a 600 h long-term stability test at 800 °C. Although the initial conductivity of Ni–ScSZ is higher than that of Ni–SASZ, it decreases to half its initial value after a 600 h measurement. On the

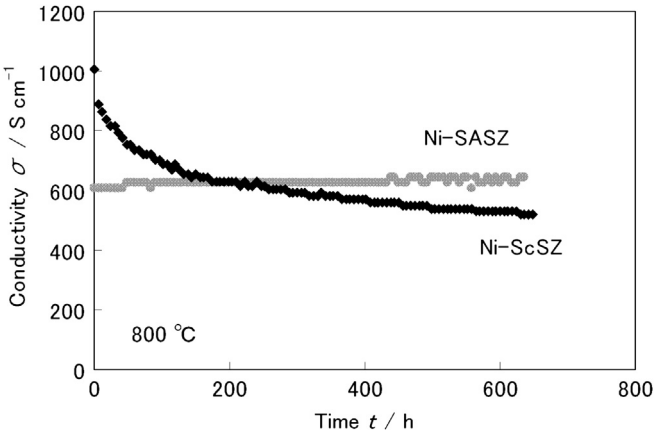

Fig. 1. Time dependence of conductivity of nickel zirconia cermets.

other hand, the conductivity of Ni–SASZ remains almost constant or increases slightly over 600 h. As regards the typical conductivity degradation behavior of nickel–zirconia cermets, it was previously reported that the conductivity decreases rapidly in the initial stage, the degradation speed then slows down, and finally reaches a constant value [22–24]. The conductivity degradation of Ni–YSZ composites in the present study corresponds to the changes in the early stages of high temperature operation and might be due to Ni particle growth at high temperatures [22]. Fig. 2 shows SEM images and the elemental distributions of the Ni in Ni–ScSZ and Ni–SASZ after a 600 h long-term stability test at 800 °C. After the 600 h test, the Ni particles were aggregated and the grains over 8 μm in size were formed in the Ni–ScSZ, whereas the Ni–SASZ maintained a fine structure with small Ni particles of about 1 μm dispersed in the cermet matrix. The reduction in Ni–ScSZ conductivity during the long-term test was caused by the aggregation of Ni in a high temperature atmosphere. The difference in the Ni aggregation during the high-temperature sintering might be due to (i) the NiO and/or zirconia particle size, (ii) the interaction strength (wettability) between Ni and zirconia, which is affected by the presence of alumina in the cermets. It has been reported that the NiO and zirconia particle sizes are important factors in the stability of the electrical conductivity [6,17]. Since our Ni–ScSZ and Ni–SASZ cermets use the same NiO powder, a similar zirconia particle size, and almost the same surface area, the effects of particle size might not be a reason for the stability difference in this case. Therefore, the additives (ii) might be a reason for the stability. Previously, the composition of the ceramic component has been reported to affect the wetting properties [19,20]. The addition of alumina to the zirconia might change the interaction and is examined in the present study.

3.2. Time dependence of conductivity of Al_2O_3 added nickel zirconia cermets

High-temperature stability was examined by measuring the conductivity changes for composite samples of NiO and ScSZ with 0.3–6 mol% of added Al_2O_3 to confirm the effect of alumina in the cermets. The porosities of the NiO–ScSZ, NiO–(97 mol% ScSZ + 3 mol% Al_2O_3), NiO–(94 mol% ScSZ + 6 mol% Al_2O_3) sintered body are 2.6%, 6.7%, 8.6%, respectively. In these samples, it seems that the porosity of NiO–zirconia sintered body increase with increasing the added Al_2O_3 amount. This might due to the small amount of Al_2O_3 act as sintering inhibitor in these samples. Fig. 3 shows the time dependence of the conductivity at 800 °C of various Ni–ScSZ samples with Al_2O_3. The initial electric

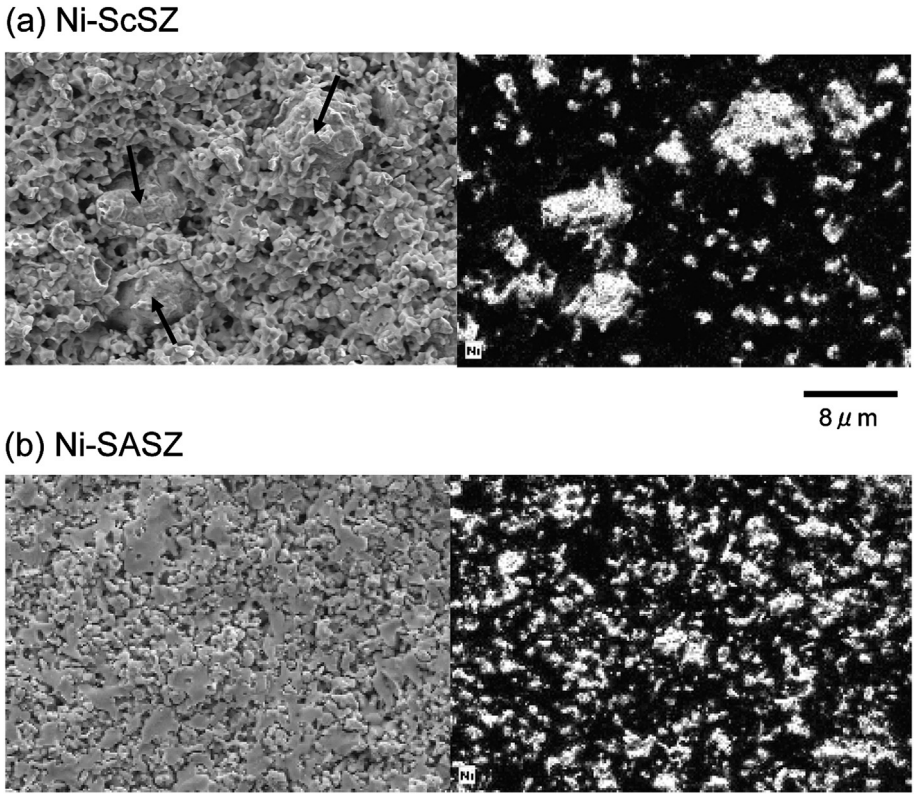

Fig. 2. SEM images of (a) Ni–ScSZ and (b) Ni–SASZ after 600 h conductivity measurement at 800 °C. The Ni distribution in the cermets was analyzed by EDS and is shown on the right. The arrows in the SEM image of (a) Ni–ScSZ show aggregated Ni particles.

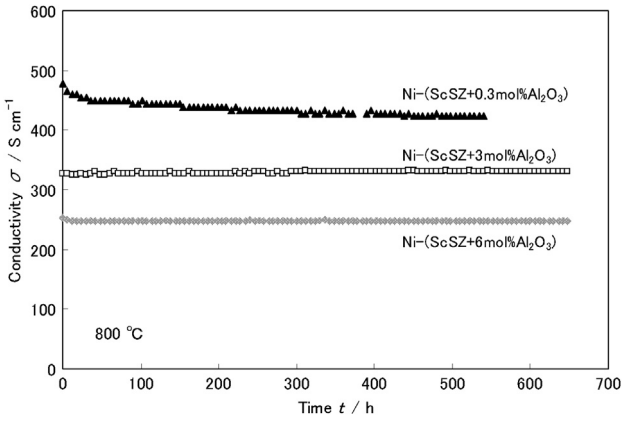

Fig. 3. Time dependence of conductivity of nickel zirconia cermets with Al_2O_3.

conductivity of the anode with Al_2O_3 decreased as the Al_2O_3 content increased. However, the anode with more than 3 mol% of Al_2O_3 maintained a constant value for over 600 h Fig. 4 shows SEM images of these Ni–ScSZ samples with Al_2O_3 after a long-term stability test at 800 °C. All the grains maintained their fine structure without any Ni aggregation after long-term operation at 800 °C.

3.3. TG analysis of anode reduction procedure

The reduction behavior of the NiO–zirconia sintered body was investigated in a reduction gas atmosphere. Fig. 5 shows TG profiles of the anodes with different compositions under CT reduction at 800 °C. The reduction curves are normalized based on the maximum value of the mass changes expected from the reduction of NiO, where a value of 1 corresponds to a full reduction to Ni metal. The reduction of NiO–SASZ and NiO–(94 mol% ScSZ + 6 mol % Al_2O_3) proceeded quickly and was almost complete after 10 or 15 min. On the other hand, the NiO–ScSZ reduction became slow after 10–20 min and complete reduction required more than 200 min. These results indicate that the anodes containing alumina exhibit faster reduction of NiO in the matrix. The microstructural differences between these composite samples could affect the anode reduction speed. Table 1 summarizes the particle size and surface area of the powdered samples, and the porosities of the sintered composites of NiO–SASZ, NiO–ScSZ, and NiO–(94 mol% ScSZ + 6 mol% Al_2O_3). The anodes containing alumina have a slightly larger porosity than the NiO–ScSZ, which is consistent with the high reduction speeds of the NiO–SASZ and NiO–(94 mol% ScSZ + 6 mol% Al_2O_3) cermets.

Yamaguchi et al. reported that the NiO conversion rate and the reaction time during the NiO reduction procedure at 240 °C are related by a sigmoid curve [25], which is characterized by an induction period followed by a steady NiO reduction, and reduction retardation occurred at higher conversion rates of over 65% [25–27]. The deviation from linear reduction behavior in the high conversion range indicates that the NiO surface is covered with Ni metal, and the metallic nickel densely deposited around NiO crystallites impedes gas diffusion into the NiO matrix [26]. On the other hand, no induction period was observed for the TG curves shown in Fig. 5 at the beginning of the reduction, because our reduction temperature of 800 °C is sufficiently high for the NiO reduction to start and proceed smoothly.

Of the three samples examined in the present study, the NiO–ScSZ composites exhibited a much slower reduction rate than the cermets containing alumina. The reduced Ni aggregates on the NiO surface of the NiO–ScSZ composites during the reduction

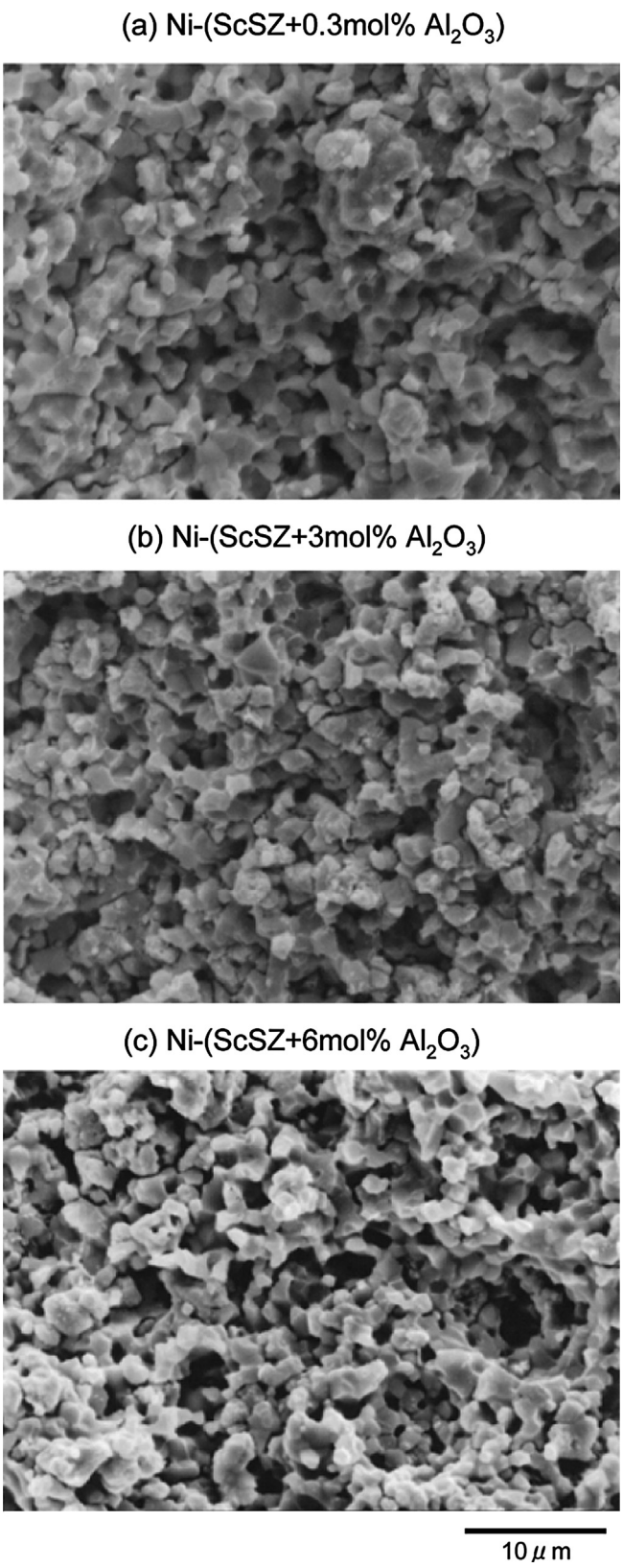

Fig. 4. SEM images of Ni–zirconia cermets with Al_2O_3 after 600 h measurement at 800 °C.

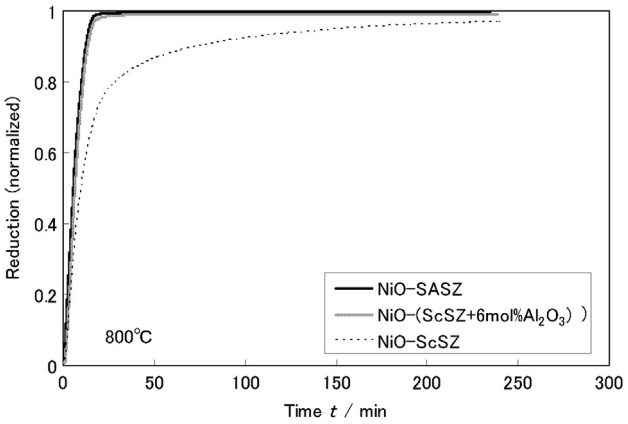

Fig. 5. TG curves of various NiO–zirconia composites under CT reduction at 800 °C.

procedure might make the reduction slower and different from those of samples containing alumina. The rapid and smooth reduction in the cermet containing alumina is consistent with there being no aggregation of the reduced Ni as seen in the SEM observation. The presence of alumina in the cermet enhances the reduction process of the NiO–zirconia composite anodes.

3.4. Reaction between NiO and Al_2O_3 at anode preparation temperature

Fig. 6 shows the XRD patterns of sintered composites of NiO–ScSZ, NiO–SASZ, NiO–(ScSZ + 6 mol% Al_2O_3). These patterns are

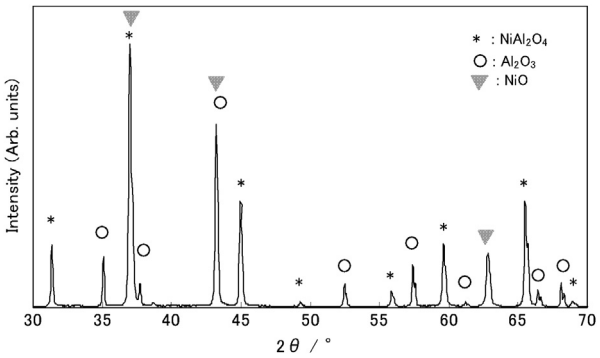

Fig. 7. XRD pattern for a mixture of NiO and Al_2O_3 heated at 1300 °C (N-A-1300).

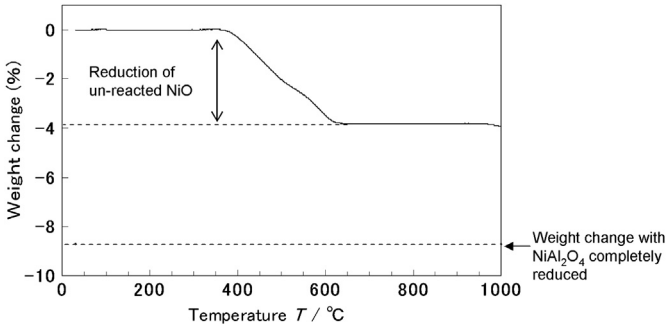

Fig. 8. TG profile of N-A-1300 under CTR reduction. The temperature ramp rate is 10 °C min^{-1}.

Table 1
Properties of NiO and zirconia powders and their composite samples.

Sample notation	Zirconia		NiO		Sintered porosity (%)
	Median particle size (μm)	Powder surface area (m^2 g^{-1})	Median particle size (μm)	Powder surface area (m^2 g^{-1})	
NiO–SASZ	0.37	10.1	3.6	0.97	6.4
NiO–ScSZ	0.53	8.9	3.6	0.97	2.6
NiO–(ScSZ-6 mol%Al_2O_3)	0.53	8.9	3.6	0.97	8.6

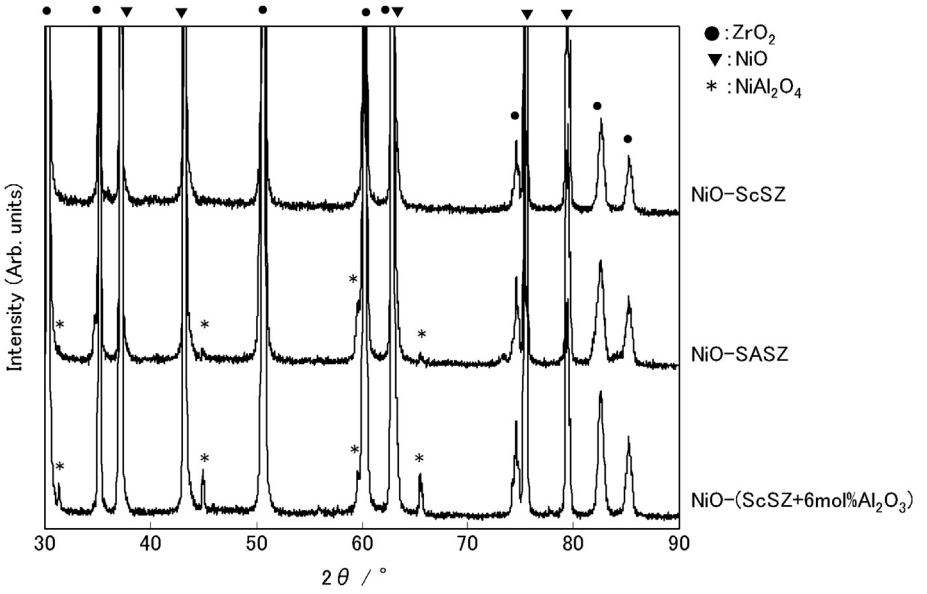

Fig. 6. XRD patterns for the as sintered anode composite samples.

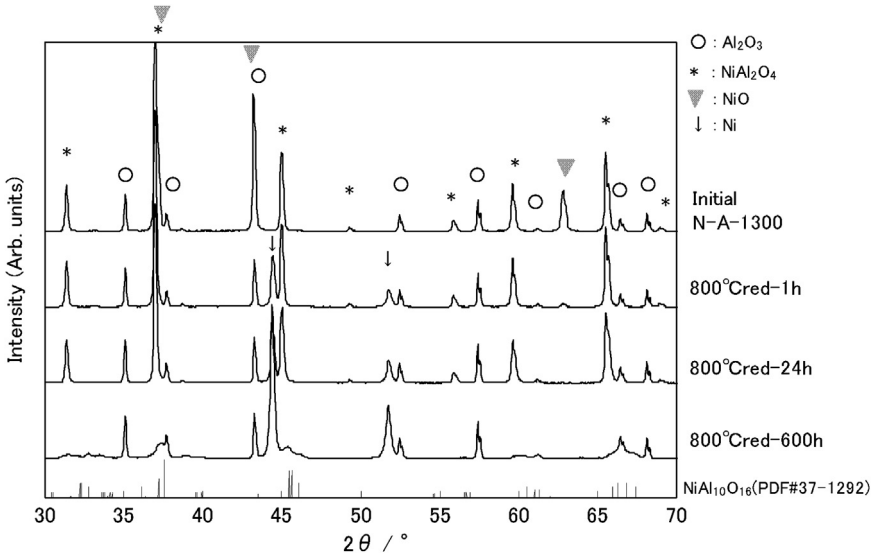

Fig. 9. XRD patterns of N-A-1300 reduced at 800 °C with various reduction times.

composed mainly of two phases, zirconia (PDF #80-2155) and NiO (PDF #89-7131). A small amount of $NiAl_2O_4$ (PDF#73-0239) was observed for the NiO–SASZ and NiO–(94 mol% ScSZ + 6 mol% Al_2O_3). The Al_2O_3 in the anode reacted with NiO during the sintering procedure and the spinel phase was formed at high temperatures. It is well known that $NiAl_2O_4$ spinel is formed by the reaction of NiO and Al_2O_3 under high temperature conditions above 1000 °C [28,29].

$$NiO + Al_2O_3 \rightarrow NiAl_2O_4 \quad (1)$$

Villa et al. reported that Al_2O_3 added to NiO induces the formation of the spinel phase ($NiAl_2O_4$) and inhibits sintering [30]. To confirm the reaction between NiO and Al_2O_3 under sample sintering conditions, NiO and Al_2O_3 powders were mixed and heated at 1300 °C for 2 h (sample: N-A-1300). Fig. 7 shows the X-ray diffraction pattern of the N-A-1300. Diffraction peaks due to $NiAl_2O_4$, NiO and Al_2O_3 are observed, and the amount of $NiAl_2O_4$ phase was found to be 43 mol% by Rietveld analysis. These results indicate that the Al_2O_3 in the cermet matrix reacts with NiO, and the interaction between NiO and Al_2O_3 might affect the stability of the anode cermets due to the formation of the spinel phase.

3.5. Reduction behavior of nickel aluminate

A TG analysis of the N-A-1300 was performed in a reduction gas atmosphere. There are two reducible oxides, NiO and $NiAl_2O_4$, in N-A-1300. The reduction reactions of these oxides are as follows.

$$NiO(solid) + H_2(gas) \rightarrow Ni(solid) + H_2O(gas) \quad (2)$$

$$NiAl_2O_4(solid) + H_2(gas) \rightarrow Ni(solid) + Al_2O_3(solid) + H_2O(gas) \quad (3)$$

Sridhar et al. reported that the activation energy of reaction (2) in the 291–509 °C range is 18 kJ mol^{-1} and that of reaction (3) in the 1014–1264 °C range is 134 kJ mol^{-1} [29]. This means that the reduction reaction of NiO (2) proceeds much more easily than that of $NiAl_2O_4$ (3).

Fig. 8 shows the TG curve obtained for N-A-1300 in a CTR reduction procedure. A 4% weight decrease from 400 to 600 °C corresponds to the reduction of the unreacted NiO. No significant weight changes were observed above 600 °C with a slight weight decrease around 1000 °C, which corresponds to the beginning of the $NiAl_2O_4$ reduction.

To confirm the reduction of $NiAl_2O_4$, phase changes under the SOFC operating condition were examined for the N-A-1300. Fig. 9 shows the XRD patterns of N-A-1300 after heating at 800 °C with various reduction times. The NiO as an unreacted phase in the initial N-A-1300 disappeared after 1 h of reduction at 800 °C. On the other hand, the $NiAl_2O_4$ phase remained after 24 h of reduction. After a 600 h reduction, the $NiAl_2O_4$ peaks at $2\theta = 31°$, 56°, 59°, and 66° disappeared and the Ni peaks at $2\theta = 44°$, and 52° increased. The pattern also shows many broad peaks around $2\theta = 30–40°$, 46° and 60–67°, which indicates the existence of $NiAl_{10}O_{16}$ (PDF#37-1292) [31]. These results show that the reduction at 800 °C proceeds very slowly from $NiAl_2O_4$ to Ni, together with the formation of $NiAl_{10}O_{16}$. It has been reported that when $NiAl_2O_4$ is reduced at low temperatures the reduction products include metastable phases that evolve prior to the formation of the equilibrium α-Al_2O_3 matrix. The metastable phase has a Ni poor composition and is called “defect spinels” [32,33]. Rod-like Ni particles have been reported to be embedded in a region identified as “defect spinels”, which are adjacent to unreacted $NiAl_2O_4$ [34,35]. The “defect spinel” phase formed in the Ni–SASZ and Ni–(ScSZ + Al_2O_3) cermet anodes after long-term reduction affects the Ni–zirconia wettability and the long-term conductivity stability of anodes with Al_2O_3.

4. Conclusion

The long term electric conductivity stability of Ni–zirconia anode under the SOFC operation condition was studied and the mechanism of the stability of Ni–SASZ was discussed. The present study is summarized as follows.

- Conductivity stability was improved and nickel aggregation was suppressed in an 800 °C reduction gas atmosphere by adding Al_2O_3 to a NiO–ScSZ anode.
- The presence of the $NiAl_2O_4$ spinel phase was confirmed from the XRD profiles of as sintered anodes with Al_2O_3.
- TG measurement under a CTR reduction condition revealed that NiO was reduced between 400 and 600 °C, whereas

$NiAl_2O_4$ was not easily reduced at an SOFC operating temperature of 800 °C.

- The $NiAl_2O_4$ spinel phase was reduced very slowly at 800 °C and was partly transformed into a meta-stable defect spinel phase of $NiAl_{10}O_{16}$ after a 600 h reduction.
- The reaction mechanism determined in the present study is as follows. A small amount of $NiAl_2O_4$ was formed at the interface of NiO and Al_2O_3 in the ScSZ during the anode sintering procedure. Once the anode was reduced, metallic Ni particles were fixed to the zirconia by the $NiAl_2O_4$ and the defect spinel phase of $NiAl_{10}O_{16}$. The composite configuration protects the aggregation of Ni particles under operating conditions, and thus provides a suitable matrix structure for the anode cermets.

Acknowledgments

We thank M. Shibata for help in preparing the composites samples, T. Ishizaki for supporting the TG measurement, and Y. Ohki for undertaking the SEM-EDS observation.

References

[1] B.W. Chung, C.N. Chervin, J.J. Haslam, A. Pham, R.S. Glass, J. Electrochem. Soc. 152 (2005) A265.
[2] F. Zhao, A.V. Virkar, J. Power Sources 141 (2005) 79.
[3] D. Waldbillig, A. Wood, D.G. Ivey, Solid State Ionics 176 (2005) 847.
[4] H. Orui, K. Nozawa, K. Watanabe, S. Sugita, R. Chiba, T. Komatsu, H. Arai, M. Arakawa, J. Electrochem. Soc. 155 (11) (2008) B1110.
[5] M. Yokoo, Y. Tabata, Y. Yoshida, H. Orui, K. Hayashi, Y. Nozaki, K. Nozawa, H. Arai, J. Power Sources 184 (2008) 84–89.
[6] T. Fukui, S. Ohara, K. Mukai, Electrochem. Solid State Lett. 1 (3) (1998) 120–122.
[7] D. Simwonis, F. Tietz, D. Stover, Solid State Ionics 132 (2000) 241–251.
[8] A. Hagen, R. Barfod, P.V. Hendriksen, Y.L. Liu, S. Ramousse, J. Electrochem. Soc. 153 (2006) A1165.
[9] S. Murakami, Y. Akiyama, N. Ishida, Y. Miyake, M. Nishioka, Y. Itoh, T. Saito, N. Furukawa, Denki Kagaku 59 (4) (1991) 320.
[10] A. Gunji, C. Wen, J. Otomo, T. Kobayashi, K. Ukai, Y. Mizutani, H. Takahashi, J. Power Sources 131 (2003) 285–288.
[11] T. Ishii, Solid State Ionics 78 (1995) 333.
[12] H. Orui, K. Watanabe, R. Chiba, M. Arakawa, J. Electrochem. Soc. 151 (9) (2004) A1412.
[13] D.W. Dees, T.D. Claar, T.E. Easlaer, D.C. Fee, F.C. Mrazek, J. Electrochem. Soc. 134 (1987) 2141.
[14] H. Koide, Y. Someya, T. Yoshida, T. Maruyama, Solid State Ionics 132 (2000) 253–260.
[15] T. Iwata, J. Electrochem. Soc. 143 (1996) 1521.
[16] C.H. Lee, C.H. Lee, H.Y. Lee, S.M. Oh, Solid State Ionics 98 (1997) 39–48.
[17] H. Itoh, T. Yamamoto, M. Mori, T. Horita, N. Sakai, H. Yokokawa, M. Dokiya, J. Electrochem. Soc. 144 (2) (1997) 641.
[18] S.P. Jiang, J. Mater. Sci. 38 (2003) 3375.
[19] A. Tsoga, P. Nikolopoulos, A. Kontogeorgakos, F. Tietz, A. Naoumides, in: Proc. SOFCV, Electrochem. Soc. Pennington, PV.97-40, 1997, 823.
[20] D. Skarmoutsos, P. Nikolopoulos, F. Tietz, I.C. Vinke, Solid State Ionics 170 (2004) 153.
[21] Y. Shiratori, Y. Teraoka, K. Sasaki, Solid State Ionics 177 (2006) 1371.
[22] M.H. Pihlatie, A. Kaiser, M. Mogensen, M. Chen, Solid State Ionics 189 (2011) 82–90.
[23] L.G. Madsen, P.H. Larsen, N. Bonanos, J. Engell, S. Linderoth, J. Mater. Sci. 41 (2006) 1097.
[24] R.J. Aaberg, R. Tunold, F.W. Poulsen, N. Bonanos, in: Proceedings of Second European SOFC Forum, vol. 1, Bernt Thorstensen, 1996, 363.
[25] A. Yamaguchi, J. Moriyama, J. Jpn. Inst. Metals 28 (1964) 692.
[26] J.T. Richardson, R. Scates, M.V. Twigg, Appl. Catal. A: Gen. 246 (2003) 137.
[27] M. Pihlatie, A. Kaiser, M. Mogensen, Solid State Ionics 180 (2009) 1100.
[28] O. Clause, B. Rebours, E. Merlen, F. Trifiro, A. Vaccari, J. Catal. 133 (1992) 231–246.
[29] S. Sridhar, D. Sichen, S. Seetharaman, Z. Metallkd. 85 (1994) 616.
[30] R. Villa, C. Cristiani, G. Groppi, L. Lietti, P. Forzatti, U. Cornaro, S. Rossini, J. Mol. Catal. A Chem. 204-205 (2003) 637.
[31] P. Bassoul, J.C. Gilles, J. Solid State Chem. 58 (1985) 383.
[32] E. Ustundag, Z. Zhang, M.L. Stocker, P. Rangaswamy, M.A.M. Bourke, S. Subramanian, K.E. Sickafus, J.A. Roberts, S.L. Sass, Mater. Sci. Eng. A238 (1997) 50–65.
[33] E. Ustundag, P. Ret, R. Subramanian, R. Dieckmann, S.L. Sass, Mater. Sci. Eng. A195 (1995) 39.
[34] E. Ustundag, R. Subramanian, R. Dieckmann, S.L. Sass, Acta Metall. Mater. 43 (1995) 383.
[35] R. Subramanian, E. Ustundag, R. Dieckmann, S.L. Sass, in: N.P. Bansal (Ed.), Advances in Ceramic Matrix Composites, Ceram. Trans. 38 (1994) 127.